Journal of Heat and Mass Transfer Research 10 (2023), Serial Number 20, 257 – 268

Journal of Heat and Mass Transfer Research

Journal homepage: https://jhmtr.semnan.ac.ir

Semnan University

ISSN: 2383-3068

esearch Article

CFD Simulation and Thermal Performance Optimization of Channel Flow with Multiple Baffles

P. Nithish Reddy [a], Vikas Verma [b], Ashwani Kumar [c], Mukesh Kumar Awasthi [* d]

[a] *Department of Mechanical Engineering, Sreenidhi Institute of Science and Technology, Hyderabad, 501301, India.*

[b] *Department of Energy, Tezpur University, Assam, 784028, India.*

[c] *Department of Mechanical Engineering, Technical Education Department Uttar Pradesh, Kanpur, 208024, India.*

[d] *Department of Mathematics, Babasaheb Bhimrao Ambedkar University, Lucknow, 226001, India.*

ARTICLE INFO

Article history:

Received: 2023-07-01

Revised: 2023-11-09

Accepted: 2023-11-09

Keywords:

CFD simulation;

Rectangular channel;

V-shaped baffles;

Turbulence

ABSTRACT

Channel flow with baffles is a multifaceted phenomenon with wide-ranging applications. It plays a crucial role in enhancing mixing, heat transfer, and other fluid dynamics processes. The baffles' design and placement within the channel are crucial to achieving the desired heat transfer enhancement. Based on the specific application and fluid properties, such as baffle geometry, spacing, and orientation must be considered. This work aims to visualize, evaluate, and understand the effectiveness of baffles on heat transfer rates under various operating conditions and design parameters. Computational Fluid Dynamic (CFD) investigations were carried out to examine the performance of channels for various geometrical configurations including Broken V-shaped, Circular, and triangular at wide operating conditions, and baffle number densities. Computational fluid dynamic (CFD) simulations were carried out for three different baffle shapes while the Reynolds number (Re) ranged from 1800 to 22000 and the no. of baffle sets(N), varied as N=15,20,30. At low Re conditions channel with 30 sets of Broken-V-shape baffles results in a higher Nusselt number due to effective turbulence enhancement and mixing in the channel. Although the thermal performance of a V-shaped baffles case is relatively good the friction factor is more for this case. Triangular baffles exhibited a lower friction factor. A maximum friction factor of 0.92 is observed for N=30 sets at Re= 1800 while the least of 0.76 is recorded for N=15.

1. Introduction

Channel baffles are vertical plates, bolted to the channel in parallel to the fluid flow path. They promote turbulence in the flow and maximize mixing efficiency [1-3]. Thus, baffles enhance the convective heat transfer rates in case of forced convection problems. The geometrical shape and baffle number play a major role in the magnitude of disturbances and accelerate the formation of turbulent structures. These structures destroy the thermal boundary growth [4-6]. The shape of the baffle plays a major role in the magnitude of turbulence in mainstream and is found to affect the performance of heat exchangers [7-9]. Raj et al. [10] performed a CFD simulation for the discretized baffle by varying the Reynolds number. The maximum enhancement was observed at a baffle angle of 60°, 0.5 cm baffle height, and 1.5 cm baffle pitch. Karima et al. [11] performed three-dimensional numerical simulations of heat exchangers with rectangular,

*** Corresponding author.**
E-mail address: mukeshiitr.kumar@gmail.com

Cite this article as:
Reddy, P. N., Verma, V., Kumar, A., Awasthi, M., 2023. CFD Simulation and Thermal Performance Optimization of Flow in a Channel with Multiple Baffles. *Journal of Heat and Mass Transfer Research*, 10(2), pp. 257-268.
https://doi.org/10.22075/JHMTR.2023.31108.1458

triangular, and circular-shaped baffles. They explored the effect on performance for a plate fin-type heat exchanger. Results show that for a circular perforated baffle, the maximum thermal performance factor was 2.14, and for a baffle, without perforation (TPF) it was 1.41. Fawaz et al. [12] carried out CFD studies for a channel flow with V-baffles at Re ranging from 5000 to 25000 for airflow. They investigated the effect of blockage ratios (BR) and pitch ratios(PR) and found that Higher BR increased the Nu. Also, a lower value of PR resulted in a better enhancement factor. Wei et al. [13] performed a CFD simulation for a channel with 90-degree V-shaped ribs. The performance of V-shaped ribs was observed to be poorer in terms of pressure drop when compared to flat channels and favorable in terms of heat transfer coefficient. Pongjet et al. [14] experimented with the performance of 60-degree V-shaped ribs in a three-dimensional channel flow. Here they placed ribs on two opposite heated walls and varied the flow Reynolds number from 10000 to 25000. They observed a maximum thermal performance of about 1.8 with BR=0.0725 which is about four times that of a flat duct without baffles at lower Re. Although many researchers explored the effect of baffles on thermal performance only a few examined the relationship between important parameters.

Wen et al. [15] investigated the effectiveness of a baffle heat exchanger with holes of different sizes. In this plate-fin heat exchanger, here max to min flow velocities dropped with a change in baffle design. They observed that improved header configuration enhances heat transfer rates to a great extent. Guo et al. [16] used the Monto-Carlo algorithm for maximization of the thermal performance of a heat exchanger. Two different types of genetic algorithms and a Monto-Carlo method are applied to find the optimum values of design and operating parameters. They reported the directions of design optimization of heat exchangers. Taler et al. [17] carried out computational fluid dynamic investigations to find the thermal contact resistance. They gave guidelines for the measurement of mean resistance for plat–fin–tube heat exchangers. In this study, they used CFD methods in the accurate prediction of fluid side and gas side temperature differences. The average heat transfer coefficient thus measured is in good agreement with the experimental results.

Jheng et al. [18] simulated channel flow with a V-shaped baffle using RNG k-ε, Realizable k-ε, and SST k-ω models. They observed that standard k−ε model results are much closer to the experimental results among the turbulent models tested. They applied a Genetic algorithm in the optimization of the thermal performance factor. Results show that GA and CFD can predict the optimum parameters, the difference in the results is only about 2 percent. Chai et al. [19] evaluated the effect of ribs in the enhancement of Nusselt number and friction factor. They observed that the ribs enhance the thermal performance compared to straight channels with a 4- 31% decrease in thermal resistance. Dogan [20] studied the thermal performance of cross-corrugated channels with rectangular baffles. They varied the segment angle and researched the effect on the Nusselt number by implementing solving numerically using a finite volume solver. They observed that the baffle of 90o angle is 52.8% more effective than the 60^{o} baffle angle in terms of Nu. A lower pressure drop of 65% was recorded at 60^{o} baffle angle configuration compared to 90^{o} angle baffle configuration. In another study, Ajeel et al. [21] evaluated the influence of geometrical parameters for trapezoidal-corrugated channels with silicon dioxide nanofluid. The results show that the (h/W) ratio has a more significant impact on heat transfer than the (p/L) ratio. The optimal parameters are h/W of 0.05 and p/L of 0.075, which significantly improve thermal performance. The trapezoidal corrugated channel with 2% silica nanofluid was found to be better than Al_2O_3 nanofluid [22]. In another study, they investigated the flow structure and heat transfer characteristics of a curved-corrugated channel with zinc oxide nanofluid. Results show that the formation of vortex flow and increased turbulence improve heat transfer rates and the best results are observed at a 10° pitch angle [23]. More experiments are carried out on the flow structure and heat transfer characteristics but with L-shaped baffles instead of E-shaped baffles. The study evaluates the effects of corrugations, baffle arrangement, corner angle, blockage ratio, Re, and ZnO particle volume fraction on performance. Results show that reducing the blockage ratio and corner angle yields the best PEC at 1.99 [24]. The use of hybrid nanofluid (CuO / MgO-water) boosted thermal performance. The thermal-hydraulic performance (THPF) increases with increasing volume fraction and Reynolds number. The best improvement is recorded at a gap ratio of 0.3 [25]. Hamad et al. [26] applied the k-ε model of turbulence in their CFD simulations of a ribbed channel flow with CuO/MgO nanofluid. Results showed that corrugations and oblique ribs increase heat transfer. Ajeel et al. [27] explore the flow in a curved-corrugated channel using CuO / MgO-water nanofluid. CFD was able to report the clear formation of the vortex and turbulent flow structures with the k-e model between the E-shaped rib structures. A similar analysis was carried out using (SiO2)-water nanofluid over Reynolds number ranges of 10,000-30,000 in a semicircle-corrugated channel and developed new correlations [28]. The study reveals that the trapezoidal corrugation profile significantly impacts heat transfer enhancement and provides better results [29]. Promvonge et al. [30] examined the performance of a solar air heater duct with a perforated rectangular wing (P-RW. The study investigates optimal P-RWs by varying attack angles and rearranging P-RWs. Results show that P-RWs increase Nusselt number (Nu) and friction factor (f) significantly over flat-plate ducts, while backward P-RWs provide the highest thermal performance. Dogan et al. [31] investigated the effect of the longitudinal and transverse pitch ratio of a vortex generator in a channel flow. The results show an inverse relation between the Nusselt number and pitch ratio, with the best results at the transverse pitch ratio of 0.12. Demirag et al. [32] carried out numerical experiments on solar air heaters fitted with conic vortex generators. The study investigated the influence of various geometric parameters and found that the highest TEF is achieved at $\alpha = 37.5°$, $\beta = 30°$, and S = 1:1. Sharma et al. [33] used triangular wing vortex generators (TWVG) for a circular tube heat exchanger. The study evaluates the impact of various flow attack angles and non-dimensional base width, han eight, and flow attack angle on the TWVG's performance. TWVG improves heat transfer through flow impingement and vortex formation, with heat transfer decreasing with increasing flow attack angle [33]. In past decade researchers have studied the discrete D-shaped ribs as artificial roughness [34], Variation in Open Area Ratio [35], Perforated multi-V ribs [36], Multi-V rib roughened [37], Multi-Parabolic Flat Plate Solar Collector [38], micro finned tubes [39] Multi-Parabolic Profile Flat-Plate Solar Collector [40] and evaluates the different parameter to enhanced the thermo-hydraulic performance of space heating-cooling devices. In his study Pachori et al. [41] have consolidated sustainable approaches for performance enhancement. Few researchers compared the performance of semicircle, trapezoidal, and straight corrugated channels. Results show that the Nusselt number and pressure drop are higher for corrugated channels than flat ones [42, 43, and 44]. Chand et al. [45] conducted a study on the influence of chemical reactions on convective double-diffusive motion within a saturated porous layer containing a viscoelastic fluid of the Kuvshiniski type using both nonlinear and linear stability techniques. Awasthi [46] investigated the impact of heat and mass transfer on instability occurring between a viscous gas and an Oldroyd B-viscoelastic liquid. Awasthi et al. [47] discussed the Rayleigh–Taylor instability at the interface between two viscous, fluids within a porous medium. This occurred in a scenario where the phases were confined between two coaxial cylindrical surfaces along with mass and heat transfer across the interface. Awasthi [48] explored the nonlinear instability at the interface of two viscous in a porous medium, there was mass and heat transfer. Yadav et al. [49] investigated the influence of chemical reactions on convective double-diffusive motion within a saturated porous layer containing a viscoelastic fluid of the Kuvshiniski type using both nonlinear and linear stability analysis.

In conclusion from the state of the art literature survey, the main objective of the current work is to do an extensive study on the effect of various baffles using CFD for a wide range of geometric and operating parameters. Geometries, like broken v-shaped, broken triangular, and broken circular shaped at different inflow velocities ranging from 0.5-6.0 m/s at a heat flux of 800W/m2, are examined. The thermal and flow characteristics are investigated and reported systematically. The broken V-baffles generated multiple pairs of longitudinal vortices in the flow path and enhanced the mixing of fluid which in turn influenced the heat transfer coefficient along the channel length. The trade-offs between different baffle shapes, such as V-shaped, triangular, or curved, in terms of their effect on flow patterns and energy dissipation, are to be understood. The geometry of baffles and their number density to maximize turbulence enhancement for improved mixing in channel flow. The influence of baffle configurations on temperature distribution and convective heat transfer rates within the channel is to be studied. Flow visualization by CFD simulation can opt to gain deeper insights into the flow behavior in channels with baffles and its effect on important parameters. Addressing these questions can lead to advancements in multiple fields of research. While there have been studies on the influence of baffle geometry on heat transfer, more research is needed to identify optimal baffle shapes, sizes, and configurations for specific applications. This includes investigating the effects of various broken baffle shapes on heat transfer enhancement. Most existing research is on high Reynolds number flows where turbulence dominates. However, many practical applications, such as low-velocity flows, operate at transitional or low Reynolds numbers. Further research is needed to understand how baffles affect heat transfer in these regimes. An attempt is made here to explore various shapes, sizes, and arrangements that maximize heat transfer and minimize friction through proper visualization using CFD study. This research aims to determine the most effective baffle shapes and geometries for specific applications. This involves studying multiple sets of broken shapes, such as circular, triangular, and broken V shapes with varying number densities, to identify which configurations yield the best heat transfer enhancement and fluid mixing [50-53].

2. Methodology

Selecting the size and shape of baffles in a channel flow system is a crucial design decision that can significantly impact heat transfer, fluid mixing, and system performance. The choice of baffle size and shape is guided by the specific objectives of the application, as well as considerations related to fluid properties, flow rates, and design constraints. The criteria and the ideas of choosing such artificial roughness growing rapidly in recent times [54-56]. In the current work, the shape and size are taken as per the following reference[18]. Figures 1, 2, and 3 shows the geometrical details of the current problem. Baffles with different geometries (broken - V, Triangular, and circular) were shown in Figures 1, 2, and 3 respectively. In the next stage, these models were meshed using the meshing tool. The length of the channel Lin = 500 mm, L(heater) = 1200 mm, Lout = 300 mm, the height H = 30 mm, and width W = 300 mm and is the same for all the cases. The thickness and height of the baffles are tb = 10 mm and h = 10 mm, respectively[18].

The flow is assumed to be a three-dimensional, steady incompressible flow with uniform inlet velocity and heat at the bottom with uniform heat flux conditions. No-slip conditions boundary conditions applied at walls and constant pressure conditions at the outlet. The standard K-e model is used to model the turbulence.

Case I: Broken V Baffles:

The CAD model of the channel with multi-broken V baffles is shown in Fig. 1(a) and Fig. 1(b). The pitch and slit distances are 35 mm and 15mm respectively (ref Fig. 1(b)).

Case II: Triangular Baffles:

The geometry of the channel with triangular baffles is shown in Fig. 2(a). The pitch and slit distances are 35 mm and 15mm respectively as shown in Fig. 2(b).

Case III: Circular Baffles:

A CAD model of the channel with Circular baffles is shown in Fig. 3(a). Slit size is again taken as 15 mm as shown in Fig. 3(b).

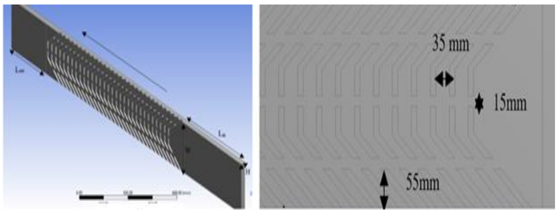

Fig. 1. CAD model of the channel with multi broken V baffles

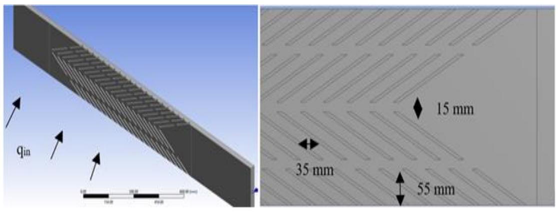

Fig. 2. Geometry of the channel with triangular baffles

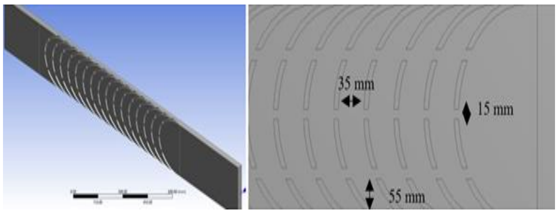

Fig. 3. Geometry of the (a) channel with circular baffles with pitch and slit distance is 35 mm and 15mm respectively

2.1. *Grid Independence Test and Validation*

Figure 4 shows the computational domain and the portion of meshed elements. Fine to medium scale sizing is done in the meshing process and the total number of elements is found to be about 3.4 Lakh to get a grid-independent result of friction factor(f) and Nusselt number(Nu). To validate the obtained results Li et al. [18] experimental results were taken as a reference to compare. Choosing broken V-shaped ,triangular, circular baffles in channel flow is often motivated by their ability to provide a balance between effective heat transfer enhancement, reduced pressure drop, and improved fluid mixing.

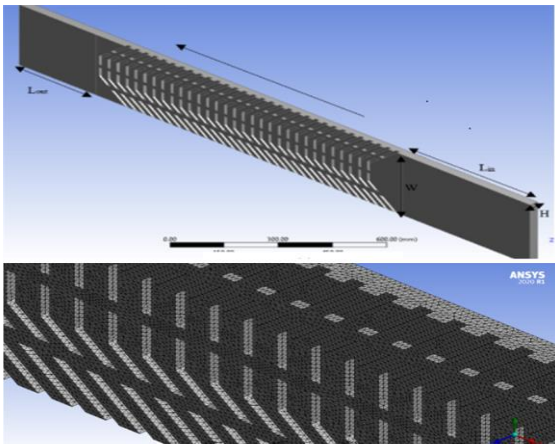

Fig. 4. Computational Doman and elements generated by meshing

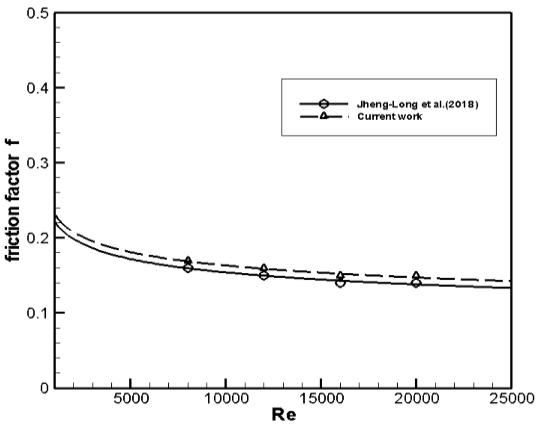

(a)

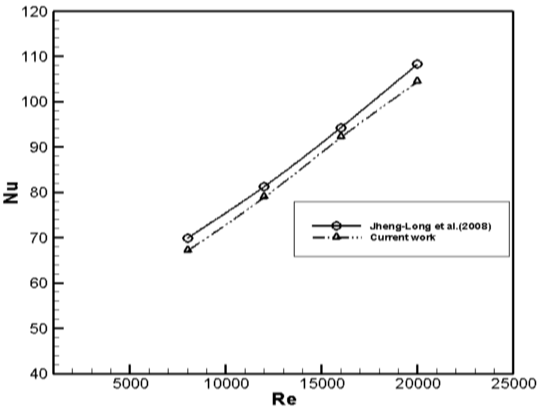

(b)

Fig. 5. Validation of current results for with that of Jheng-Long [18]: (a) f vs Re; (b) Nu vs Re. at α=60°, Pr=2, e/H=0.3.

The unique size of broken spaced baffles and the different number densities offers several advantages in certain applications. Several numerical experiments were conducted related to each in order to deeply examine the effect of number density of baffle sets of different broken geometrical configurations. Figure 5 shows the comparison of current results for the friction factor (f) and Nu with that of Li et al. [18] . Here the Nu and f are compared in the case of a v-shaped baffle. Results are presented for four different Re 8000, 12000, 16000, and 20000, from the chart it can be seen that the variation is less than 5% in each case. Thus, further analysis is carried out for other geometries.

3. Results and Discussion

In this work, numerical experiments on channel flow with baffles set of different geometries were carried out by using a finite-volume solver. Steady-state forced convective investigations were carried out for five different velocities between 0.5 – 6 m/s (corresponding Re= 1800 to 22000) and with a bottom heat source of 800 W/m². Here Nu and friction factor f were compared for all the models considered.

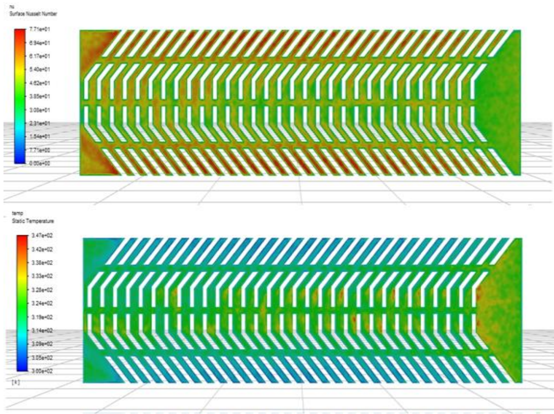

Fig. 6. Nu contour (top) and Temperature contour (bottom) at 6 m/s velocity and 800 W/m² heat flux

Figure 6 shows the base case contours of the Nusselt number, surface temperature for broken v-shaped baffles corresponding to 6 m/s velocity, and 800 W/m² heat flux. For modeling turbulence, the k-ε model is applied, and second-order accurate schemes are used for discretization. It can be seen in Fig. 6(a) that at 800 W/m² and 6m/s velocity, the surface Nusselt number at the heater was 55.99. Also, it can be noted that the average surface temperature rises (ref. Fig. 6b) from 300K to 347K at 800 W/m² at 6m/s velocity due to steady-state heating and convective heat transfer.

Figures 7 and 8 give a comparison of thermal contours with variation in inlet flow Reynolds number for the selected three baffle shapes and different baffle densities respectively. From the contours (ref. Fig. 7) it can be observed that the surface temperatures are relatively low in each case concerning V-shaped baffles followed by circular baffles.

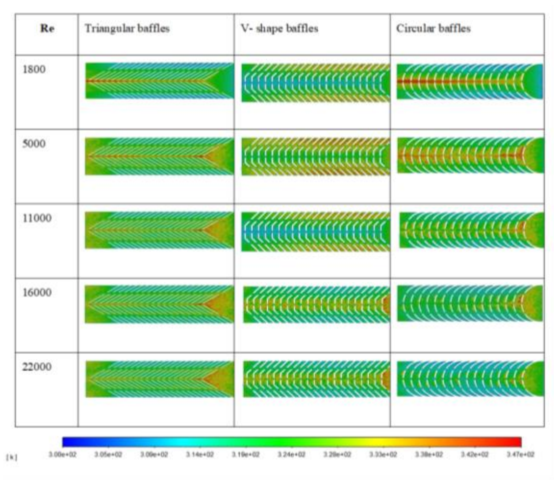

Fig. 7. Temperature contour with a variation of Re vs. Shape of baffles.

The difference is high when the Reynolds number is high compared to the low Reynolds number and a difference of about 8 degrees is noticed. This could be due to enhanced turbulence factor and higher flow Reynolds number when encountering a baffle. Thus, it can be said here that is V-shaped baffle as shown in the figure is relatively more effective in generating turbulence in the channel flow.

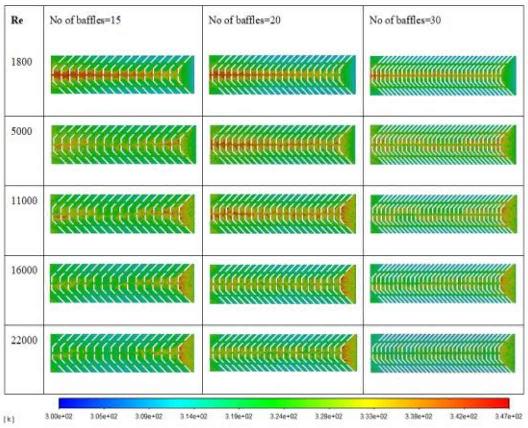

Fig. 8. Temperature contour with a variation of Re vs. the number of baffles

Figure 8 shows the effect of baffles number on the surface temperature decreased with Re as a result of increased convection rates. The temperature is on almost equal levels with the change in the count of baffles, which shows the effect is relatively low. At lower Re higher number of baffles recorded lower temperatures whereas at higher Reynolds numbers lower number of baffles is found to be suitable. On average about 334 ^{o}C observed at Re=1800 while the temperature is about 322^{o}C at Re= 22000.

Figures 9 and and 10 give a comparison of streamlines with variation in inlet flow Reynolds number for the selected three types of baffles geometries and number of baffles respectively.

Figure 9 presents the streamlines and their pattern concerning Triangular, V-shaped, and circular baffles. The flow patterns are different in each case but the common in each case is that the flow turns turbulent as it passes through the baffles. From the figure (ref. fig. 9) it can be seen that flow is initially straight-lined and then it turns random with different patterns as they start passing through baffles.

A similar phenomenon is also seen in Figure 10 where the effect of baffles density or change in the number of baffles is presented.

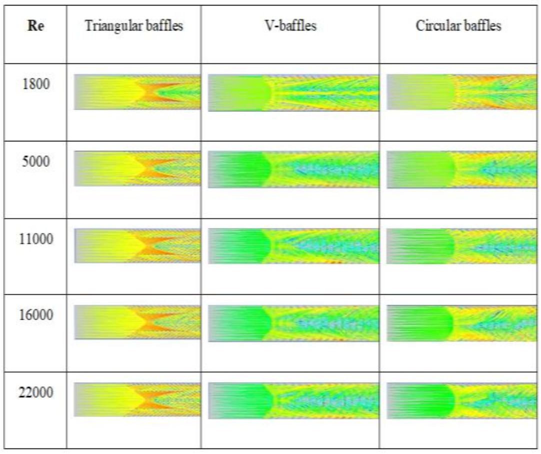

Fig. 9. Streamlines with a variation of Re vs. Shape of baffles

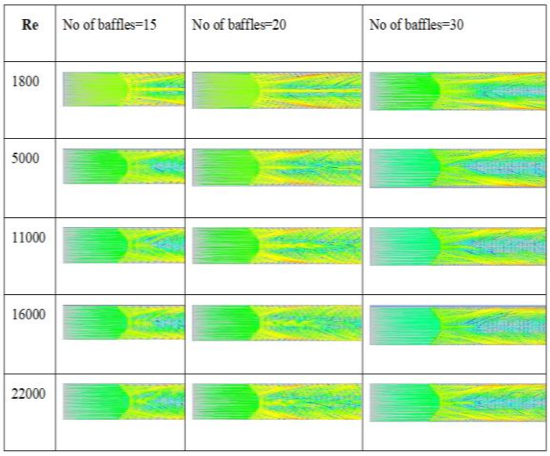

Fig. 10. Streamlines with a variation of Re vs. the number of baffles.

Figures 11 and and 12 give a comparison of the Nusselt number with variation in inlet flow Reynolds number for the selected three baffle shapes and baffle numbers respectively. Figure 11 gives a comparison of the Nu contour for the three configurations chosen; results show that the Nu enhances with the Re which can be seen through an increase in red indication in the contour. The higher side of the local Nusselt number here is about 77.1 and the same can be seen through the legend underneath the figure. On average the Nusselt number is about 45 for triangular baffles and as high as 55 for V-shaped baffles at Re=22000 But the difference found less significant at Re=1800.

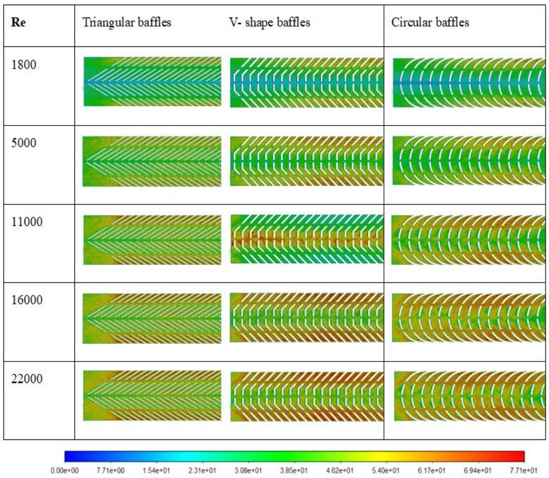

Fig. 11. Nusselt Number with a variation of Re vs. Shape of baffles

Figure 12 shows the effect of the number of baffles on the Nu in the case of a V-shaped configuration. From the figure, it can be seen that a lower Re side n=30 showed better Nu values while a higher Re side n=15 is found to be more effective. This can be attributed to the fact that at lower velocities more baffles are required to generate turbulence while at higher velocities a few can do the job.

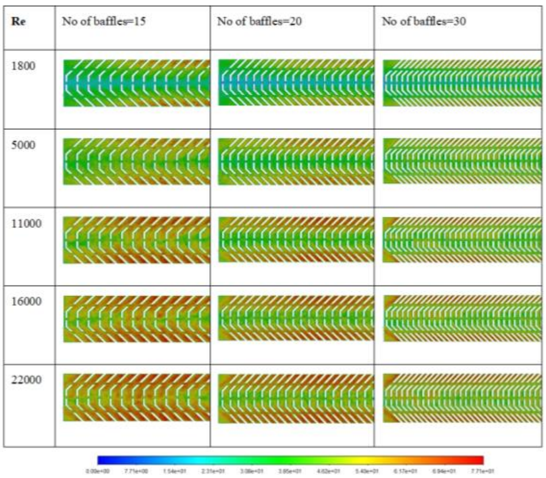

Fig. 12. Nusselt Number with a variation of Re vs. the number of baffles

Figure 13 shows Reynold's number augmentation led to Nusselt number enhancement due to forced convection effects in all three cases.

From Fig. 13, it can be observed that the Re showed a positive effect on Nu. V-shaped baffles case recorded the highest Nu. In all three sets of baffles, at lower velocities, the Nusselt number is nearly equal for all the geometries, as the velocities increase the Nusselt number increases in broken V-shape baffle due to the vortex flow. These vortices hamper the boundary layer growth and thus enhance the convective heat transfer rates.

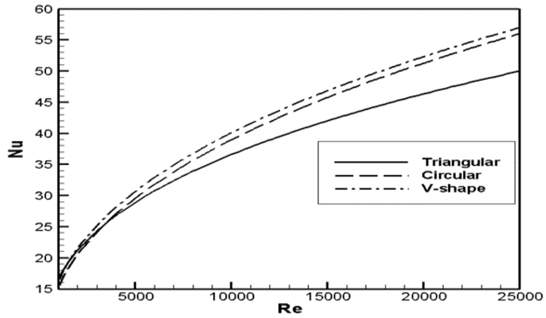

Fig. 13. Nu vs. Re for different geometries of baffles

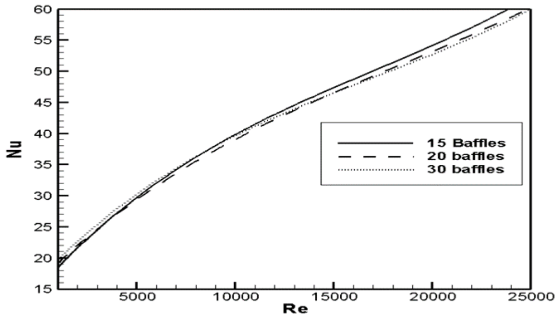

Fig. 14. Nu vs. Re for different sets of V-shape baffles

Figure 14 represents the comparison of Surface Nusselt number (Nu) contours of V-shaped geometric configuration for a different number of baffle sets. Fig. 14 shows the highest Nusselt number for 15 sets of baffles at higher Re, whereas the Nusslet number is slightly high for 30 sets in the case of lower Re. In all three sets of baffles, a small difference in the Nusselt number is noticed as the Re increases. More baffles can enhance disturbance, and record powerful turbulence but it is equally important to provide proper spacing in between to sustain the turbulence. Otherwise, the number of baffle sets may not be as effective as intended.

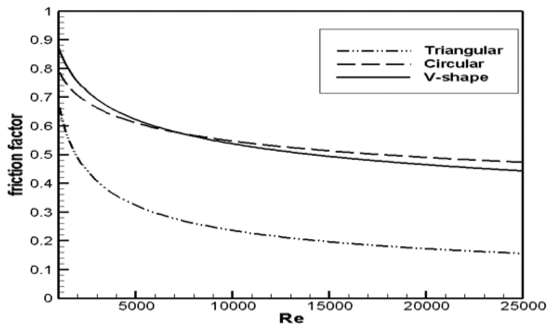

Fig. 15. f vs. Re for different geometries of baffles

The effect of the Re on the friction factor(f) for three cases is shown in Fig. 15. The friction factor(f) decreased slightly with an increase in Re, for the V-shaped case and circular baffles case reported high friction factor when compared to triangular baffles. The lowest friction factor is reported in triangular baffle sets because the streamlined geometrical shape reduces the resistance significantly and reduces energy consumption. Whereas a V-shaped baffle case has reported relatively greater flow disturbances due to its blunt front portion.

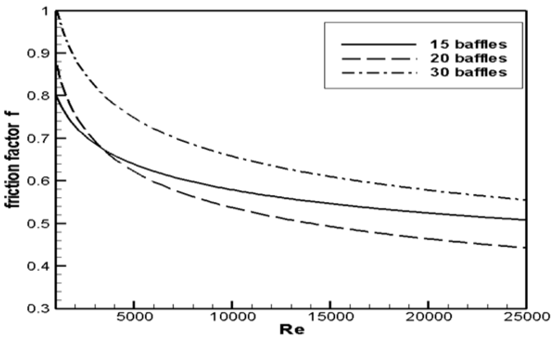

Fig. 16. f vs. Re for different sets of V-shape baffles

The effect of the Re on the 'f' for different baffle sets is presented in Fig. 16. Friction factor(f) decreases with the increase in Re, and it is noted that 30 no. of baffle sets case has a higher 'f' than the other cases. The lowest friction factor was recorded with the case of 20 no. of baffle sets at higher Re and 15 number sets at lower Re. This phenomenon may be due to enhanced turbulence at higher Re may lead to lower pressure drop and thus lower friction coefficients.

In all the cases friction loss increased although the heat transfer improved. Therefore, it is important to evaluate the Thermal Enhancement Factor (TEF) in this field [36]. TEF is calculated as the ratio of the heat transfer coefficient of the augmented surface to that of the smooth surface at equal pumping power. The thermal enhancement factor or the efficiency of the introduced ribs is calculated by using the below equation[57-58]. The thermo hydraulic performance parameter or enhancement factor is calculated as

$$\eta = \frac{\left(\frac{Nu}{Nu_o}\right)}{\left(\frac{f}{f_o}\right)^{0.33}} \tag{1}$$

Figure 17 presents the variation in thermal enhancement factor concerning the Reynolds number for different geometries. From the plot, it can be observed that the TEF initially increases in all the cases with an increment in Reynolds number and then decreases gradually. This initial increment can be due to the transition from laminar to turbulent regime with a change in Reynolds number. Maximum TEF is recorded with Triangular baffles followed by V-shaped baffles and the least is noted with Circular Baffles. The important observation is that the TEF is always above 1.0 which ensures economic viability.

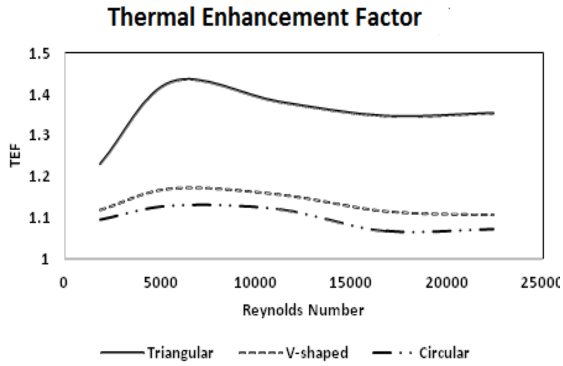

Fig. 17. TEF vs. Reynolds number plot for different baffle shapes

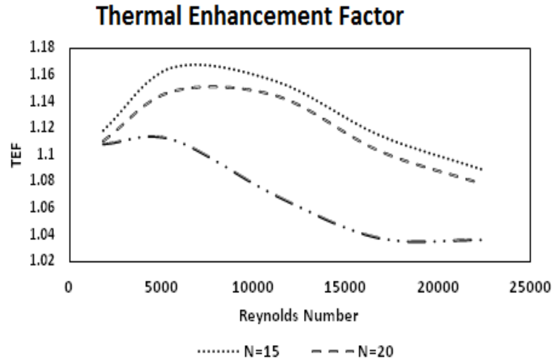

Fig. 18. TEF vs. Reynolds number at different baffle number(N)

In Figure 18 as the number of baffles is increased from 15 to 30 the TEF is reduced and the peak value of TEF is noticed in the transition regime for all the cases with these V-shaped baffles. Here it clearly shows that although the heat transfer rates are influenced by the increase in baffles, the baffle density also has a major effect on Nu and Friction factors. Thus, it is recommended to use the baffles optimally for a good thermal enhancement factor.

Metal baffles can be manufactured by using machining, laser cutting, water jet cutting, stamping, or welding to create the desired baffle shapes. In case of Composite baffles, can opt for layup and curing processes. Multiple baffles can be placed in channel by following means. Based on the spacing and number, baffles can be welded, bolted, or fastened in place, depending on the material and application. Surface treatments could include painting, anodizing, or applying corrosion-resistant coatings [59-61].

4. Conclusions

Channels with baffles, often referred to as baffled channels, find applications in various industrial and scientific processes. Three-dimensional investigations were carried out on the turbulent thermal performance of a channel flow under different baffle configurations. The effect of operating parameters like Reynolds number and geometric parameters on three types of baffle shapes and configuration densities are examined. The impacts of the above inputs on the friction factor(f) and Nusselt number(Nu) are investigated and recorded. Results show that:

- The average surface temperatures recorded are high for circular-shaped baffles for all Reynolds numbers among all three shapes. The channel with V-shape baffles showed a higher Nusselt number when compared to the other two geometric configurations.
- A maximum average Nusselt number of 56.46 is recorded for V-shaped baffles at Re=22000 and the least of 20.82 is recorded for circular baffles at Re=1800. At a lower Reynolds number, more baffle sets generate effective turbulence while at a higher Reynolds number, few baffles could do.
- The friction factor(f) reduced with the Re and it augmented with an increase in the baffle set count(N). At N=30 highest friction factor is recorded. A maximum friction factor of 0.92 is observed for N=30 sets at Re= 1800 while the least of 0.76 is recorded for N=15.
- Although the thermal performance of the V-shaped baffles case is relatively good the friction factor is more for this case. Triangular baffles exhibited a lower friction factor.
- At Re= 1800 maximum friction factor of 0.81 is recorded for the V-shaped baffle while the least of 0.54 is recorded for Triangular baffles. At higher Re i.e. at 22000, the friction factor is below 0.5 for all three cases.
- Thermal Enhancement factor is found to be better in the case of triangular baffles and its value is high in transition regime.

Nomenclature

D	hydraulic diameter (mm)
E	baffle height(mm)
F	friction factor
H	height of channel (mm)
Nu	Nusselt number
W	channel width (mm)
L	channel Length
A	angle of the V-shape baffle
M	dynamic viscosity (N·s/m^2)
P	density (kg/m^3)
CFD	Computational fluid dynamics
p	pressure (Pa)
P	baffle pitch (mm)
q	heat flux (W/m^2)
Re	Reynolds number
T	Temperature (°K)
tb	thickness of the baffle

Subscripts

n	inlet
out	Outlet
b	Baffle
o	smooth channel

Conflicts of Interest

The author declares that there is no conflict of interest regarding the publication of this manuscript. In addition, the authors have entirely observed the ethical issues, including plagiarism, informed consent, misconduct, data fabrication and/or falsification, double publication and/or submission, and redundancy.

References

[1] Ameur, H., 2019. Effect of the baffle inclination on the flow and thermal fields in channel heat exchangers. *Results in Engineering*, 3, p.100021.

[2] Abrofarakh, M. and Moghadam, H., 2023. Numerical study on thermo-hydraulic performances of hybrid nanofluids flowing through a corrugated channel with metal foam. *Journal of heat and mass transfer research*, 10(1), pp.147-158.

[3] Rana, S., Kumar, A., 2018. FEA Based Design and Thermal Contact Conductance Analysis of Steel and Al Rough Surfaces. *International Journal of Applied Engineering Research (IJAER)*, Volume 13, Number 16, pp. 12715-12724, ISSN 0973-4562.

[4] Kumar, A., Saini, R.P. and Saini, J.S. ,2012. Experimental investigation on heat transfer and fluid flow characteristics of airflow in a rectangular duct with Multi V-shaped rib with gap roughness on the heated plate. *Solar Energy*, 86, pp.1733–1749.

[5] Moon, M., Park, M. and Kim, K. ,2014. Evaluation of heat transfer performances of various rib shapes. *Journal of Heat and Mass Transfer*, 71, 275–284

[6] Ajibade, A. Ojeagbase, P.O., 2020. Effect of viscous dissipation on steady natural convection heat and mass transfer in a vertical channel with variable viscosity and thermal conductivity. *Journal of Heat and Mass Transfer*, 7(2),pp. 105-116.

[7] Mith, E., Arnut, P., Khwanchit, W., Monsak, P., Naoki, M. and Masafumi, H. ,2023. Thermal

evaluation of flow channels with perforated-baffles. *Energy Reports*, 9, 525–532.

[8] Li, Z., Sun, S., Wang, C., Liang, C., Zeng, S., Zhong, T., Hu, W. and Feng, C. ,2022. The effect of trapezoidal baffles on heat and flow characteristics of a cross-corrugated triangular duct. *Case Studies in Thermal Engineering*, 33, p.101903.

[9] Dash, A.P., Alam, T., Siddiqui, M.I.H., Blecich, P., Kumar, M., Gupta, N.K., Ali, M.A. and Yadav, A.S., 2022. Impact on heat transfer rate due to an extended surface on the passage of microchannel using cylindrical ribs with varying sector angle. *Energies*, 15(21), p.8191.

[10] Raj, K., Ranchan, C., Muneesh, S. and Anil, K., 2017. Experimental study and correlation development for Nusselt number and friction factor for discretized broken V-pattern baffle solar air channel. *International Journal of Thermal Sciences*, 81, pp.56–75.

[11] Karima, B., Houari, A., Djamel, S. and Mohamed, B., 2016. Effect of the perforation design on the fluid flow and heat transfer characteristics of a plate-fin heat exchanger. *Experimental Thermal and Fluid Science*, 126, pp. 0894–1777.

[12] Fawaz, H.E., Badawy, M.T.S., AbdRabbo, M.F. and Amr, E., 2017. Numerical investigation of fully developed periodic turbulent flow in a square channel fitted with 450 in-line V-baffle turbulators pointing upstream. *Alexandria Engineering Journal*, 57(2), pp.633-642.

[13] Peng, W., Jiang, P.X., Wang, Y.P. and Wei, B.Y., 2011. Experimental and numerical investigation of convection heat transfer in channels with different types of ribs. *Applied Thermal Engineering*, *31*(14-15), pp.2702-2708.

[14] Pongjet, P., Wayo, C., Sutapat, K. and Chinaruk, T., 2011. Numerical heat transfer study of turbulent square-duct flow through inline V-shaped discrete ribs. *International Communications in Heat and Mass Transfer*, 38, pp.1392–1399.

[15] Wen, J. and Li, Y., 2004. Study of flow distribution and its improvement on the header of plate- fin heat exchanger. *Cryogenics*, 44, pp. 823–831.

[16] Guo, D., Liu, M., Xie, L. and Wang, J., 2014. Optimization in plate-fin safety structure of heat exchanger using genetic and Monte Carlo algorithm. *Applied Thermal Engineering*, 70, pp.341–349.

[17] Taler, D. and Ocłoń, P., 2014. Thermal contact resistance in plate fin-and-tube heat exchangers, determined by experimental data and CFD simulations. *International Journal of Thermal Sciences*, 84, pp. 309–322.

[18] Li, J.L., Tang, H.W. and Yang, Y.T., 2018. Numerical simulation and thermal performance optimization of turbulent flow in a channel with multi V-shaped baffles. *International Communications in Heat and Mass Transfer*, *92*, pp.39-50.

[19] Chai, L. and Wang, L., 2018. Thermal-hydraulic performance of interrupted microchannel heat sinks with different rib geometries in transverse microchambers. *International Journal of Thermal Sciences*, 127, pp. 201–212.

[20] Dogan, E.A., 2020. Thermohydraulic performance study of different square baffle angles in the cross-corrugated channel. *Journal of Energy Storage*, 28, p.101295.

[21] Ajeel, R.K., Salim, W.S.-I.W. and Hasnan, K., 2019. Influences of geometrical parameters on the heat transfer characteristics through symmetry trapezoidal-corrugated channel using SiO2-water nanofluid. *International Communications in Heat and Mass Transfer*, 101, pp. 1–9.

[22] Ajeel, R.K., Saiful-Islam, W., Sopian, K. and Yusoff, M.Z., 2020. Analysis of thermal-hydraulic performance and flow structures of nanofluids across various corrugated channels: An experimental and numerical study. *Thermal Science and Engineering Progress*, 19, p.100604.

[23] Ajeel, R.K., Sopian, K. and Zulkifli, R., 2021. A novel curved-corrugated channel model: Thermal-hydraulic performance and design parameters with nanofluid. *International Communications in Heat and Mass Transfer*, 120, pp. 105037.

[24] Ajeel, R.K., Sopian, K. and Zulkifli, R., 2021. Thermal-hydraulic performance and design parameters in a curved-corrugated channel with L-shaped baffles and nanofluid. *Journal of Energy Storage*, 34, p.101996.

[25] Ajeel, R.K., Zulkifli, R., Sopian, K., Fayyadh, S.N., Fazlizan, A. and Ibrahim, A., 2021. Numerical investigation of binary hybrid nanofluid in new configurations for curved-corrugated channel by thermal-hydraulic performance method. *Powder Technology*, 385, pp.144–159.

[26] Hamad, A.J. and Ajeel, R.K., 2022. Combined effect of oblique ribs and a nanofluid on the thermal-hydraulic performance of a corrugated channel: Numerical study. *Journal of Engineering Physics and Thermophysics*, 95, pp. 970–978.

[27] Ajeel, R.K., Sopian, K., Zulkifli, R., Fayyadh, S.N. and Kareem Hilo, A.K., 2021. Assessment and analysis of binary hybrid nanofluid impact on new configurations for curved-corrugated channel. *Advanced Powder Technology*, 32, pp. 3869–3884.

[28] Ajeel, R.K., Salim, W.S.-I.W. and Hasnan, K., 2019. Design characteristics of symmetrical semicircle-corrugated channel on heat transfer enhancement with nanofluid. *International Journal of Mechanical Sciences*, 151, pp.236–250.

[29] Ajeel, R.K., Salim, W.S.-I., Sopian, K., Yusoff, M.Z., Hasnan, K., Ibrahim, A. and Al-Waeli, A.H.A., 2019. Turbulent convective heat transfer of silica oxide nanofluid through corrugated channels: An experimental and numerical study. *International Journal of Heat and Mass Transfer*, 145, p.118806.

[30] Promvonge, P. and Skullong, S., 2019. Heat transfer augmentation in solar receiver heat exchanger with hole-punched wings. *Applied Thermal Engineering*, 155, pp.59–69.

[31] Dogan, M. and Erzincan, S., 2023. Experimental investigation of thermal performance of novel type vortex generator in rectangular channel. *International Communications in Heat and Mass Transfer*, 144, p.106785.

[32] Demirağ, H.Z., Doğan, M. and İğci, A.A., 2023. The experimental and numerical investigation of novel type conic vortex generator on heat transfer enhancement. *International Journal of Thermal Sciences*, 191, p.108383.

[33] Sharma, V.R., S, S.S., N, M. and M S, M., 2022. Enhanced thermal performance of tubular heat exchanger using triangular wing vortex generator. *Cogent Engineering*, 9(1).

[34] Dutt, N., Hedau, A.J., Kumar, A., Awasthi, M.K., Singh, V.P. and Dwivedi, G., 2023. Thermo-hydraulic performance of solar air heater having discrete D-shaped ribs as artificial roughness. *Environmental Science and Pollution Research*, pp. 1-22.

[35] Singh, V.P., Jain, S., Karn, A., Dwivedi, G., Alam, T. and Kumar, A., 2023. Experimental Assessment of Variation in Open Area Ratio on Thermohydraulic Performance of Parallel Flow Solar Air Heater. *Arab J Sci Eng*, 48, pp. 11695–11711.

[36] Singh, V.P., Jain, S., Karn, A., Dwivedi, G., Kumar, A., Mishra, S., Sharma, N.K., Bajaj, M., Zawbaa, H.M. and Kamel, S., 2022. Heat transfer and friction factor correlations development for double pass solar air heater artificially roughened with perforated multi-V ribs. *Case Studies in Thermal Engineering*, *39*, p.102461.

[37] Singh, V.P., Jain, S., Kumar, A., 2023. Establishment of correlations for the thermo-hydraulic parameters due to perforation in a multi-V rib roughened single pass solar air heater. *Experimental Heat Transfer*, 36(5), pp.597-616.

[38] Dutt, N., Kumar, R. and Murugesan, K. 2023. Experimental Performance Analysis of Multi-Parabolic Flat Plate Solar Collector. In: Li, X., Rashidi, M.M., Lather, R.S., Raman, R. (eds) Emerging Trends in Mechanical and Industrial Engineering. Lecture Notes in Mechanical Engineering. *Springer*, Singapore.

[39] Singh, A.R., Solanki, A.K. and Dutt, N., 2023. Heat transfer and pressure drop penalty study in flattened micro-finned tubes. In *Advances in Mathematical and Computational Modeling of Engineering Systems* (pp. 279-293). CRC Press.

[40] Verma, V., 2021. Optimization of Multi-Parabolic Profile Flat-Plate Solar Collector for Space-Heating Application. In *Advances in Energy Technology: Proceedings of ICAET 2020* (pp. 189-201). Springer Singapore. https://doi.org/10.1007/978-981-15-8700-9_18.

[41] Pachori, H., Baredar, P., Sheorey, T., Gupta, B., Verma, V., Hanamura, K. and Choudhary, T.,2023. Sustainable approaches for performance enhancement of the double pass solar air heater equipped with energy storage system: A comprehensive review, Journal of Energy Storage, 65, p.107358.

[42] Ajeel, R.K., Salim, W.S.-I.W. and Hasnan, K., 2019. Experimental and numerical investigations of convection heat transfer in corrugated channels using alumina nanofluid under a turbulent flow regime. *Chemical Engineering Research and Design*, 148, pp. 202–217.

[43] Ajeel, R.K., Salim, W.S.-I.W. and Hasnan, K., 2019. Thermal performance comparison of various corrugated channels using nanofluid: Numerical study. *Alexandria Engineering Journal*, 58, pp. 75–87.

[44] Eiamsa-ard, S., Phila, A., Wongcharee, K., Pimsarn, M., Maruyama, N. and Hirota, M., 2023. Thermal evaluation of flow channels with perforated-baffles. *Energy Reports*, *9*, pp.525-532.

[45] Reddy, N. and Murugesan, K., 2018. Numerical Study of Vorticity and Heat Flow in Bottom Heated DDC Systems at Nominal Rayleigh Number. *Journal of Applied Fluid Mechanics*, *11*(2), pp.309-322.

[46] Awasthi, M,K., Dutt, N., Kumar, A., Kumar, S., 2023. Electrohydrodynamic capillary instability of Rivlin–Ericksen viscoelastic fluid film with mass and heat transfer. *Heat Transfer*. pp.1-19.

[47] Chandra, A. S., Reddy, P. N. and Rajan, H., 2022. Natural ventilation in a lege space with heat source: CFD visualization and taguchi optimization. *Journal of Thermal Engineering,* 8(5), pp.642-655.

[48] Awasthi, M. K., 2014. Nonlinear analysis of capillary instability with mass transfer through porous media. *The European Physical Journal Plus*, *129*, pp.1-11.

[49] Yadav, D., Awasthi, M. K., Al-Siyabi, M., Al-Nadhairi, S., Al-Rahbi, A., Al-Subhi, M., Ragoju, R., and Bhattacharyya, K., 2022. Double diffusive convective motion in a reactive porous medium layer saturated by a non-Newtonian Kuvshiniski fluid. *Physics of Fluids*, *34*(2).

[50] Saha, A.C., Verma, V., Tarodiya, R., Mahboob, M.R., Kumar, R., 2021. Analytical modeling of a radiant cooling system for thermal performance analysis. *Materials Today: Proceedings,* 47(10), pp. 2474-2480.

[51] Reddy, N., and Murugesan, K., 2016. Numerical Study of Double-Diffusive Convection in a Heated Lid-Driven Cavity with Mass Diffusive Side Walls. *Computational Thermal Sciences: An International Journal*, *8*(4), pp.381-398.

[52] Reddy, N., Murugesan, K., 2017. Finite element study of DDNC in bottom heated enclosures with mass diffusive side walls. Frontiers in heat and mass transfer, 8, pp.1-11.

[53] Thangavel, S., Verma, V., Tarodiya, R., Kaliyaperumal, P., 2021. A study on optimization of horizontal ground heat exchanger parameters for space heating application. *Materials Today: Proceedings,* 47(10), pp. 2293-2298.

[54] Kumar, R., Kumar, S., Nadda, R., Kumar, K. and Goel, V., 2022. Thermo-hydraulic efficiency and correlation development of an indoor designed jet impingement solar thermal collector roughened with discrete multi-arc ribs. *Renewable Energy,* 189, pp. 1259-1277,

[55] Kumar, R., Nadda, R., Kumar, S., Saboor, S., C. Saleel, C., Abbas, M., Afzal, A. and Linul E., 2023. Convective heat transfer enhancement using impingement jets in channels and tubes: A comprehensive review. *Alexandria Engineering Journal*, 70, pp.349-376.

[56] Kumar, R., Nadda, R., Rana, A., Chauhan, R., Chandel, S.S., 2020. Performance investigation of a solar thermal collector provided with air jets impingement on multi V-shaped protrusion ribs absorber plate. Heat Mass Transfer 56, 913–930. https://doi.org/10.1007/s00231-019-02755-2.

[57] Kumar, R., Kumar, R., Kumar, S., Thapa, S., Sethi, M., Fekete, G. and Singh, T., 2022. Impact of artificial roughness variation on heat transfer and friction characteristics of solar air heating system. *Alexandria Engineering Journal*, 61(1), pp.481-491.

[58] Kumar R., Rahul Nadda, Kumar S., Razak A., Sharifpur M, Hikmet S. Aybar, C Ahamed S. and Asif A., 2022. Influence of artificial roughness parametric variation on thermal performance of solar thermal collector: An experimental study, response surface analysis and ANN modelling. *Sustainable Energy Technologies and Assessments*, 52, pp. 102047

[59] Singh, S., Behura, S.K., Kumar, A. and Verma, K. eds., 2022. *Nanomanufacturing and Nanomaterials Design: Principles and Applications*. CRC Press.

[60] Kumar, A., Kumar, A. and Kumar, A., 2023. Introduction to Optics and Laser-Based Manufacturing Technologies. In *Laser-based Technologies for Sustainable Manufacturing* (pp. 1-43). CRC Press.

[61] Dewangan, A.K., Moinuddin, S.Q., Cheepu, M., Sajjan, S.K., Kumar, A., 2023. Thermal Energy Storage: Opportunities, Challenges and Future Scope. *In Thermal Energy Systems: Design, Computational Techniques and Applications* (pp. 17-28). CRC Press.